

Constraints on eustatic sea-level changes during the Mid-Pleistocene Climate Transition : Evidence from the Japanese shallow-marine sediment record

メタデータ	言語: en 出版者: Elsevier 公開日: 2018-03-19 キーワード (Ja): キーワード (En): 作成者: Kitamura, Akihisa メールアドレス: 所属:
URL	<a href="http://hdl.handle.net/10297/00024834">http://hdl.handle.net/10297/00024834</a>

25 Constraints on eustatic sea-level changes during the Mid-Pleistocene

26 Climate Transition: evidence from the Japanese shallow-marine sediment record

27 Akihisa Kitamura

28 *Institute of Geosciences, Shizuoka University, 836 Oya, Suruga-ku, Shizuoka, 422-8529, Japan*

29

30 ABSTRACT

31 During the Middle Pleistocene, the nature of glacial–interglacial fluctuations changed from  
32 low-amplitude and a periodicity of 41 kyr to high-amplitude and quasi-periodic of 100 kyr. The  
33 origin of the Mid-Pleistocene Climate Transition (MPT) is an unsolved mystery. At present,  
34 there is a debate about whether the initiation of the MPT was a gradual or an abrupt process.  
35 This study investigated the process of initiation of the MPT from reconstructions of eustatic  
36 sea-level changes, as a proxy for global ice volume, based on a reexamination of lithofacies and  
37 fossil occurrences from shallow-marine sediments (the Omma Formation) exposed on the west  
38 coast of Japan. The Omma Formation comprises 19 depositional sequences spanning marine  
39 isotope stages (MIS) 56–21.3, reflecting sedimentation under alluvial plain to offshore  
40 conditions. The data indicate that (1) sea-level was lowest during MIS 22 (~0.9 Ma); (2)  
41 sea-level during MIS 34 (~1.13 Ma) and MIS 26 (~0.96 Ma) was lower than during any other  
42 glacial stage, except for MIS 22; and (3) sea-level during MIS 22 was at most 20 m lower than  
43 during MIS 34 and 26. Together, these findings suggest that the initiation of the MPT was a  
44 gradual, rather than abrupt, process.

45

## 46 **1. Introduction**

47 Glacial–interglacial cycles, and corresponding changes in eustatic sea-level, have had a  
48 considerable impact on both global climate and ecosystems throughout the Quaternary. Between

49 2.7 and 1.2 Ma, these cycles occurred with a periodicity of 41 kyr (the “41-kyr world”), and are  
50 attributed primarily to changes in the Earth’s obliquity (Raymo and Nisancioglu, 2003; Huybers,  
51 2006). In contrast, for the past 0.7 Myr, glacial cycles have followed an approximately 100-kyr  
52 periodicity (the “100-kyr world”) (Hays et al., 1976; Imbrie et al., 1992). The timing of the  
53 glacial–interglacial cycles is explained by the theory postulated by Milankovitch in the early  
54 20th century, which changes in boreal summer insolation are responsible for changes in the  
55 volume of boreal glacial ice sheets. However, the transition from the 41-kyr to the 100-kyr  
56 world, termed the Mid-Pleistocene Climate Transition (MPT) (e.g., Pisias and Moore, 1981),  
57 appears to bear no relation to orbital forcing. Furthermore, there is little agreement as to when  
58 the MPT occurred.

59 Clark et al. (2006) suggested that the constructed LR04 “stacked” benthic  $\delta^{18}\text{O}$  record  
60 (Lisiecki and Raymo, 2005) (Fig. 1) shows the MPT beginning at ~1.25 Ma with a gradual  
61 increase in global ice volume and decrease in deep-water temperature. This hypothesis was  
62 supported by Sosdian and Rosenthal (2009), who reconstructed early Pleistocene eustatic  
63 sea–level (and hence global ice volume) changes with orbital-scale resolution using changes in  
64 the  $\delta^{18}\text{O}$  of seawater based on analyses of  $\delta^{18}\text{O}$  and Mg/Ca ratios of the epifaunal benthic  
65 foraminifera *Cibicidoides wuellerstorfi* and *Oridorsalis umbonatus* from North Atlantic Deep  
66 Sea Drilling Project (DSDP) site 607 (Fig. 1). However, Yu and Broecker (2010) questioned the  
67 result of Sosdian and Rosenthal (2009), because of the confounding influence of carbonate ion  
68 saturation on epifaunal benthic foraminiferal Mg/Ca ratios.

69 Recently, Elderfield et al. (2012) provided a record of eustatic sea–level for the past 1.5  
70 Myr from Ocean Drilling Program (ODP) 181, site 1123, off New Zealand (Fig. 1). The record,  
71 based on  $\delta^{18}\text{O}$  and Mg/Ca ratios of the shallow-infaunal benthic foraminifera *Uvigerina* spp.  
72 (the shells of which are barely affected by carbonate-ion saturation), suggests that the MPT was

73 initiated by an abrupt increase in Antarctic ice volume at MIS 22 (~0.9 Ma). According to  
74 Elderfield et al. (2012), the uncertainty of the sea-level changes are  $\pm 20$  m. More recently,  
75 Rohling et al. (2014) reconstructed eustatic sea-level changes over the past 5.3 Myr using  
76 eastern Mediterranean planktonic foraminiferal  $\delta^{18}\text{O}$  records. The authors reported a strong  
77 agreement between their reconstruction and the sea-level estimates of Elderfield et al. (2012),  
78 although the 95% probability interval of the Rohling et al. (2014) is  $\pm 6.3$  m.

79 Prior to these studies, Bintanja et al. (2005) reconstructed the sea-level curve during the  
80 past 1.1 Myr from an ice-sheet-ocean-temperature model and the LR04 “stacked” benthic  $\delta^{18}\text{O}$   
81 record (Lisiecki and Raymo, 2005), although they did not discuss the pattern of initiation of the  
82 MPT. According to Bintanja et al. (2005), the uncertainty of their sea-level changes is  $\pm 10$  m.

83 Consequently, independent constraints on sea-level during the early Pleistocene glacial  
84 periods are required to help determine whether the initiation of the MPT was a gradual or an  
85 abrupt process. As the upper limits of U/Th dating and polar ice cores records are 0.5 Ma and  
86 0.8 Ma, respectively, shelfal and nearshore sedimentary records provide useful constraints on  
87 eustatic sea-level changes during the early Pleistocene.

88 Existing shallow-water sediment records include those of the Wanganui Basin in New  
89 Zealand (Beu and Edwards, 1984; Abbott and Carter, 1994; Carter and Naish, 1998; Kondo et  
90 al., 1998), the Croton Basin in southern Italy (Rio et al., 1996; Massari et al., 1999, 2011), the  
91 Merced Formation in northern California (Carter et al., 2002), the Seoguipo Formation in  
92 southern Korea (Kim et al., 2010), and collisional marine foreland basin of southern Taiwan  
93 (Chen et al., 2001) (Fig. 1). However, because these marine basins are too deep to detect small  
94 fluctuations in sea-level, none of these previous studies identified depositional sequences that  
95 correspond to MIS 22–24 in their lithostratigraphic schemes. In contrast, the depositional  
96 sequence in the Omma Formation, Central Japan, is firmly correlated with MIS 55–21

97 (Kitamura and Kawagoe, 2006) (Fig. 2) and thus encompasses this transitional period. To  
98 investigate the process of initiation of the MPT, this study reconstructed eustatic sea-level  
99 changes in glacial period, as a proxy for global ice volume, based on a reexamination of  
100 lithofacies and fossil occurrences from the Omma Formation.

101

## 102 **2. Geological setting of depositional sequences in the Omma Formation**

103 The Omma Formation is exposed around Kanazawa City, along the west coast of Central  
104 Japan (Fig. 1). The formation is up to 220 m thick in the type section along the Saikawa River at  
105 Okuwa. The Omma Formation overlies the middle Miocene Saikawa Formation (Ogasawara,  
106 1977) and is in turn overlain unconformably by the Utatsuyama Formation (Ichihara et al.,  
107 1950) (Fig. 2). The marine Saikawa Formation is mainly composed of massive siltstone  
108 (Ogasawara, 1977). The Utatsuyama Formation is about 100 m thick and comprises fan-delta  
109 deposits of alternating beds of mudstone, coarse-grained sandstone, and conglomerate (Nirei,  
110 1969).

111 Biostratigraphic and magnetostratigraphic data (Takayama et al., 1988; Ohmura et al.,  
112 1989; Sato and Takayama, 1992; Kitamura et al., 1994) indicate that the basement of the Omma  
113 Formation at the type section is located between the first occurrence (FO) of *Gephyrocapsa*  
114 *oceanica* ( $1.664 \pm 0.025$  Ma; Berger et al., 1994) and the FO of *Gephyrocapsa* (large) ( $1.515 \pm$   
115  $0.025$  Ma; Berger et al., 1994) (Fig. 2). These data show that the top of the formation is located  
116 below the Brunhes–Matuyama magnetic polarity reversal (Fig. 2).

117 The Omma Formation has been divided into lower, middle, and upper parts (Fig. 2)  
118 (Kitamura et al., 1994, 2001). The lower and middle parts consist of 14 depositional sequences  
119 (Fig. 2, L1–L3, M1–11) that include the following architectural elements, in ascending  
120 stratigraphic order: (1) a basal sequence boundary that is superposed on the ravinement surface;

121 (2) a transgressive systems tracts (TST) (2–5 m thick) consisting of a basal shell bed of 0.3 m  
122 thick (a condensed onlap shell bed) overlain by fine- to very-fine-grained sandstone; (3) a  
123 maximum flooding horizon coinciding with the horizon with the highest concentration of  
124 sand-size carbonate grains; (4) a highstand systems tracts (HST) (2–3 m thick) consisting of  
125 fine-grained sandstone and sandy siltstone; and (5) a regressive systems tracts (RST) (<1 m  
126 thick) comprising fine-grained sandstone with a coarsening-upward trend (Kitamura et al.,  
127 2000). The upper part of the formation consists of five depositional sequences (Fig. 2, U1–U5)  
128 associated with back-marsh to inner-shelf environments (Kitamura and Kawagoe, 2006). Erect  
129 stumps and tracks of elephants and deers have been found from back-marsh deposits (Kitamura  
130 and Kawagoe, 2006). These parts of the Omma Formation show no progressive shift in litho-  
131 and biofacies toward deeper or shallower deposits.

132       Except for four depositional sequences in the upper part, during the deposition of each  
133 sequence, the molluscan fauna changed from cold-water, upper-sublittoral species to  
134 warm-water, lower-sublittoral species, followed by a return to cold-water, upper-sublittoral  
135 species (Kitamura et al., 1994). The term “cold-water species” is applied to fauna living in the  
136 area north of southern Hokkaido and/or in water deeper than 150–160 m off Sanin and  
137 Hokuriku. These species are present in the Pacific coast area north of the Boso Peninsula at  
138 35°N, where the warm Kuroshio Current diverges away from the Japanese Islands. The term  
139 “warm-water species” is applied to fauna living in the area south of southern Hokkaido, and  
140 living at the area shallower than 150–160 m depth off Sanin and Hokuriku. The area off Sanin  
141 and Hokuriku is strongly influenced by the warm Tsushima Current, which is a branch of the  
142 warm Kuroshio Current. These species are present south of 35°N on the Pacific coast of Japan.  
143 The cyclic changes in molluscan content in these depositional sequences indicate that ocean  
144 conditions and water depth fluctuated concurrently. Specifically, increased water depths

145 correspond to periods of warmer marine conditions associated with the inflow of the warm  
146 Tsushima Current. Thus, the depositional sequences of the Omma Formation are correlated with  
147 obliquity-driven glacio-eustatic changes, with a periodicity of 41 kyr (Kitamura et al., 1994).  
148 Kitamura and Kimoto (2006) correlated 19 depositional sequences in the Omma Formation with  
149 oxygen isotope stages 56 to 21.3 using a combination of sequence stratigraphic, biostratigraphic,  
150 and magneto stratigraphic data (Fig. 2). As noted above, the Omma Formation contains only  
151 shallow-marine facies that can be perfectly correlated between oxygen isotope stages and  
152 depositional sequences during MIS 55–21.

153

### 154 **3. Sea-level reconstruction**

155 Water depth in sedimentary basins can be influenced by several factors, including  
156 compaction, basement subsidence, sediment supply, hydro-isostatic effects, and eustatic  
157 sea-level changes. The basement rock on which the Omma Formation was deposited (i.e., the  
158 Saikawa Formation sediments) was consolidated prior to deposition of the Omma Formation,  
159 since the lower unconformity is penetrated by marine rock-boring bivalves (Kitamura, 1997).  
160 The sediments of the Omma Formation are unconsolidated and consist primarily of very-fine- to  
161 fine-grained sandstone, with a burial depth equal to the total formation thickness (210 m). From  
162 the porosity–depth relationship (Sclater and Christie, 1980; Ramm and Bjiørlykke, 1994),  
163 sandstone porosity within the formation decreases by only 5% from the surface to a burial depth  
164 of 250 m, indicating that the water–depth curve is only weakly affected by compaction.

165 With the exception of depositional sequence U4 (DS U4), which corresponds to MIS  
166 22–21.4 (Kitamura and Kawagoe, 2006), the sequence boundaries for the depositional  
167 sequences of the Omma Formation coincide with ravinement surfaces formed by shoreface  
168 erosion during marine transgression (Bruun, 1962). As the depth of shoreface erosion is

169 generally less than 40 m (e.g., Saito, 1989), water depths at sequence boundaries probably  
170 remained at least than 40 m for the 800-kyr period between MIS 56 and 21.3, indicating that  
171 basin subsidence kept pace with sediment supply.

172       Being located far from the former continental ice-sheets, the marine basin of the Omma  
173 Formation was influenced by hydro-isostasy alone, in which rising (falling) sea-level causes  
174 basin subsidence (uplift) due to increasing (decreasing) water load. Consequently, relative  
175 sea-level during glacial periods can be compared directly, allowing water-depth changes  
176 represented by the Omma Formation to be used as a proxy for eustatic sea-level changes.

177       Water depth change, as recorded by the Omma Formation, has been reconstructed by  
178 analyses of lithofacies and fossil occurrences (Kitamura, 1991; Kitamura et al., 1994; Kitamura  
179 and Kawagoe, 2006; Kitamura and Kimoto, 2006) (Fig. 2). Non-marine sediments, comprising  
180 back-marsh deposits found in the lowest levels of DS U4 (MIS 22), suggest that sea-level  
181 during MIS 22 was lower than at any other time between MIS 56 and 21 (Kitamura and  
182 Kawagoe, 2006). Kitamura and Kimoto (2004) and Kitamura and Kawagoe (2006) described  
183 well-sorted, fine-sand units that contain parallel laminations or hummocky cross-stratification in  
184 the upper levels of depositional sequences 8 and U1, corresponding to MIS 36–34 and 28–26,  
185 respectively (Fig. 2). These sediments do not contain fossils such as molluscs and foraminifera,  
186 due to the dissolution of calcareous shell materials. Sedimentary structures indicate that the  
187 sediments were deposited in a lower shoreface environment. Because the fair-weather wave  
188 base lies at depths of about 5–15 m (Walker and Plint, 1992), the depth of the lower shoreface is  
189 inferred to be 5–15 m. The reexamination herein indicates that, with the exception of MIS 22,  
190 sea-level was lower during MIS 34 (~1.13 Ma) and 26 (~0.96 Ma) than during any other glacial  
191 stage between MIS 56 and 21.

192

193 **4. Discussion and conclusion**

194 Based on a reexamination of lithofacies and fossil occurrences from the shallow-marine  
195 Omma Formation, sea-level was lower during MIS 22 than at any other time between MIS 56  
196 and 21. This finding is in close agreement with the findings of Bintanja et al. (2005), Elderfield  
197 et al. (2012), and Rohling et al. (2014), and supports the argument for a significant increase in  
198 global ice volume at MIS 22, referred to by Clark et al. (2006) as the 900-ka event.

199 This reexamination also indicates that sea-level was lower during MIS 34 and 26 than  
200 during other glacial stages (except for MIS 22) of the same time period, in agreement with the  
201 conclusion of Bintanja et al. (2005). According to Elderfield et al. (2012) and Rohling et al.  
202 (2014), sea-level in MIS 34 and 26 was not significantly lower than in the other glacial periods  
203 between MIS 56 and 21. This is inconsistent with the new evidence of the present study.

204 The differences in sea-level between MIS 22 and the two glacial stages MIS 34 and 26 are  
205 estimated to have been 20 m (Bintanja et al., 2005), 40 m (Rohling et al., 2014) or 50 m  
206 (Elderfield et al., 2012) (Fig. 2). As noted above, the water depth is thought to have been  
207 between 5 and 15 m during MIS 34 and 26. Conversely, the sea-level during MIS 22 is  
208 uncertain, because the study area emerged and was a back-marsh environment during this period  
209 (Fig. 2). When the difference in sea-level of 50 m (20 m) is applied, the elevation of the study  
210 area is estimated to have been 35–45 m (5–15 m) during MIS 22. As back-marsh commonly  
211 develops in low coastal plains, it is likely that the difference in sea-level was 20 m, as  
212 determined by Bintanja et al. (2005), rather than the 40–50 m estimated by Elderfield et al.  
213 (2012) and Rohling et al. (2014).

214 As noted above, the uncertainties in estimates of sea-level from geochemical data range  
215 from  $\pm 6.3$  m to  $\pm 20$  m (Bintanja et al., 2005; Elderfield et al., 2012; Rohling et al., 2014). In  
216 contrast, as hydrographic conditions change drastically from shoreface to offshore, lithofacies

217 are highly sensitive to changes in sea-level during sea-level low stands. It is therefore likely  
218 that the inconsistency between this study and the geochemical studies of Elderfield et al. (2012)  
219 and Rohling et al. (2014) reflect uncertainties in the estimates from geochemical data.

220 This means that the early Pleistocene sea-level curve of Bintanja et al. (2005) is more  
221 suitable than those of Elderfield et al. (2012) and Rohling et al. (2014), and that the initiation of  
222 the MPT was a gradual (e.g., Clark et al., 2006), rather than abrupt, process (Elderfield et al.,  
223 2012).

224

## 225 **Acknowledgments**

226 I thank three anonymous reviewers, whose comments and suggestions improved the original  
227 manuscript.

228

## 229 **References**

- 230 Abbott, S.T., Carter, R.M., 1994. The sequence architecture of mid-Pleistocene (0.35–0.95 Ma)  
231 cyclothem from New Zealand: facies development during a period of orbital control on  
232 sea-level cyclicity. In: de Boer, P.L., Smith, D.G. (Eds.), *Orbital Forcing and Cyclic  
233 Sequences*. International Association of Sedimentologist Special Publication 19, 367–394.
- 234 Berger, W.H., Yasuda, M.K., Bickert, T., Wefer, G., Takayama, T., 1994. Quaternary time scale  
235 for the Ontong Java Plateau: Milankovitch template for Ocean Drilling Program Site 806.  
236 *Geology* 22, 463–467.
- 237 Beu, A.G., Edwards, A.R., 1984. New Zealand Pleistocene and late Pliocene glacio-eustatic

238 cycles. *Palaeogeography, Palaeoclimatology, Palaeoecology* 46, 119–142.

239 Bintanja, R., van de Wal R.S.W., Oerlemans, J., 2005. Modelled atmospheric temperatures and  
240 global sea levels over the past million years. *Nature* 437, 125–128.

241 Bruun, P., 1962. Sea level rise as a cause of shoreface erosion. *Journal of the Waterways and  
242 Harbors Division: proceedings of the American Society of Civil Engineers* 88, 117–130.

243 Carter, R.M., Naish, T.R., 1998. A review of Wanganui Basin, New Zealand: global reference  
244 section for shallow marine, Plio-Pleistocene (2.5-0 Ma) cyclostratigraphy. *Sedimentary  
245 Geology* 122, 37–52.

246 Carter, R.M., Abbott, S.T., Graham, I.J., Naish, T.R., Gammon, P.R., 2002. The middle  
247 Pleistocene Merced-2 and -3 sequences from Ocean Beach, San Francisco, *Sedimentary  
248 Geology* 153, 23–41.

249 Chen, W.S., Ridgway, K.D., Horng, C.S., Chen, Y.G., Shea, K.S., Yeh, M.G., 2001. Stratigraphic  
250 architecture, magnetostratigraphy, and incised-valley systems of the Pliocene-Pleistocene  
251 collisional marine foreland basin of Taiwan. *Geological Society of America Bulletin* 113,  
252 1249-1271.

253 Clark, P.U., Archer, D., Pollard, D., Blum, J.D., Rial, J.A., Brovkin, V, Mix, A.C., Pisias, N.G  
254 and Roy, M., 2006 The middle Pleistocene transition: characteristics, mechanisms, and  
255 implications for long-term changes in atmospheric pCO<sub>2</sub>. *Quaternary Science Reviews* 25,

256 3150–3184.

257 Elderfield, H., Ferretti, P., Greaves, M., Crowhurst, S., McCave, I.N., Hodell, D., Piotrowski,  
258 A.M., 2012. Evolution of ocean temperature and ice volume through the mid-Pleistocene  
259 climate transition. *Science* 337, 704–709.

260 Hays, J.D., Imbrie, J., Shackleton, N.J., 1976. Variations in the Earth’s orbit: pacemaker of the  
261 ice ages. *Science* 194, 1121–1132.

262 Huybers, P., 2006. Early Pleistocene glacial cycles and the integrated summer insolation  
263 forcing. *Science* 313, 508–511.

264 Ichihara, M., Ishio, G., Morishita, A., Nakagawa, T., Tsuda, K., 1950. Geological study of  
265 the Toyama and Ishikawa Prefectures. No. 2, Kanazawa, Isurugi and Fukumitsu provinces.  
266 *Chigaku* 2, 17–27 [in Japanese].

267 Imbrie, J., Boyle, E.A., Clemens, S.C., Duffy, A., Howard, W.R., Kukla, G., Kutzbach, J.,  
268 Martinson, D.G., McIntyre, A., Mix, A.C., Molino, B., Morley, J.J., Peterson, L.C., Pisias,  
269 N.G., Prell, W.L., Raymo, M.E., Shackleton, N.J., Toggweiler, J.R., 1992. On the structure  
270 and origin of major glaciation cycles. 1. Linear responses to Milankovitch forcing.  
271 *Paleoceanography* 7, 701–738.

272 Kim, J.K., Khim, B.-K., Woo, K.S., Yoon, S.H. 2010: Records of palaeo-seawater condition  
273 from oxygen-isotope profiles of early Pleistocene fossil molluscs from the Seoguipo

274 Formation (Korea). *Lethaia* 43, 170–181.

275 Kitamura, A., 1991. Paleoenvironmental transition at 1.2 Ma in the Omma Formation, Central  
276 Japan. *Transactions and Proceedings of the Palaeontological Society of Japan*. 162, 767–  
277 780.

278 Kitamura, A., 1997. The lower unconformity and molluscan fossils of the basal part of the early  
279 Pleistocene Omma Formation at its type section, Ishikawa Prefecture, central Japan. *The*  
280 *Journal of the Geological Society of Japan* 103, 763–769 [Japanese with English abstract].

281 Kitamura, A., 1998, Glaucony and carbonate grains as indicators of the condensed section:  
282 Omma Formation, Japan. *Sedimentary Geology* 122, 151–163.

283 Kitamura, A., Kondo, Y., Sakai, H., Horii, M., 1994, Cyclic changes in lithofacies and content in  
284 the early Pleistocene Omma Formation, Central Japan related to the 41,000-year orbital  
285 obliquity. *Palaeogeography, Palaeoclimatology, Palaeoecology* 112, 345–361.

286 Kitamura, A., Matsui, H., Oda, M., 2000. Constraints on the timing of systems tract  
287 development with respect to sixth-order (41 ka) sea-level changes: an example from the  
288 Pleistocene Omma Formation, Sea of Japan. *Sedimentary Geology* 131, 67–76.

289 Kitamura, A., Takano, O., Takada, H., Omote, H., 2001, Late Pliocene-early Pleistocene  
290 paleoceanographic evolution of the Sea of Japan. *Palaeogeography, Palaeoclimatology,*  
291 *Palaeoecology* 172, 81–98.

292 Kitamura, A., Kawagoe, T., 2006, Eustatic sea-level change at the mid-Pleistocene climate  
293 transition: New evidence from the Japan shallow-marine sediment record. *Quaternary*  
294 *Science Review* 25, 323–335.

295 Kitamura, A., Kimoto, K., 2006. History of the inflow of the warm Tsushima Current into the  
296 Sea of Japan between 3.5 and 0.8 Ma. *Palaeogeography, Palaeoclimatology, Palaeoecology*

297 236, 355–366.

298 Kondo, Y., Abbott, S.T., Kitamura, A., Naish, T., Kamp, P.J.J., Kamataki, T., Saul, G.S., 1998.

299 The relationship between shellbed type and sequence architecture: Examples from Japan and

300 New Zealand. *Sedimentary Geology* 122, 109–127.

301 Lisiecki, E.L., Raymo, E.R., 2005, A Pliocene-Pleistocene stack of 57 globally distributed

302 benthic  $\delta^{18}\text{O}$  records. *Paleoceanography* 20, PA1003, doi:10.1029/2004PA001071.

303 Massari, F., Sgavetti, M., Rio, D., D' Alessandro, A., Prosser, G., 1999. Composite sedimentary

304 record of falling stages of Pleistocene glacio-eustatic cycles in a shelf setting (Croton basin,

305 south Italy). *Sedimentary Geology* 127, 85–110.

306 Massari, F., Rio, D., Sgavetti, M., Prosser, G., D'Alessandro, A., Asioli, A., Capraro, L.,

307 Fornaciari, E., Tateo, F., 2011. Interplay between tectonics and glacio-eustasy: Pleistocene

308 succession of the Croton basin, Calabria (southern Italy). *Geological Society of America*

309 *Bulletin* 114, 1183–1209.

310 Nirei, H., 1969. On the Utatsuyama Formation around Kanazawa City, Central Japan. *The*

311 *Journal of the Geological Society of Japan* 75, 471–484 [in Japanese with English abstract].

312 Ogasawara, K., 1977. Paleontological analysis of Omma Fauna from Toyama-Ishikawa area,

313 Hokuriku Province, Japan. *Science Reports of the Tohoku University, Second Series,*

314 *Geology* 47, 43–156.

315 Ohmura, I., Ito, T., Masaeda, H., Danbara, T., 1989. Magnetostratigraphy of the Omma

316 Formation distributed in Kanazawa City, Ishikawa Prefecture, central Japan. Professor H.  
317 Matsuo Memoir 111-124 [Japanese with English abstract].

318 Piasias, N.G., Moore, Jr., T.C., 1981. The evolution of Pleistocene climate: a time series  
319 approach. *Earth and Planetary Science Letters* 52 450–458.

320 Ramm, M., Bjørlykke, K., 1994. Porosity/depth trends in reservoir sandstones: Assessing the  
321 quantitative effects of varying pore-pressure, temperature history and mineralogy,  
322 Norwegian Shelf Data. *Clay Minerals* 24, 475–490.

323 Raymo, M.E., Nisancioglu, K., 2003. The 41 kyr world: Milankovitch's other unsolved mystery.  
324 *Paleoceanography* 18, doi:10.1029/2002PA000791.

325 Rio, D., Channell, J.E.T., Massari, F., Poli, M.S., Sgavetti, M., D'Alessandro, A., Prosser, G.,  
326 1996. Reading Pleistocene eustasy in a tectonically active siliciclastic shelf setting (Crotone  
327 peninsula, southern Italy). *Geology* 24, 743–746.

328 Rohling, E.J., Foster, G.L., Grant, K.M., Marino, G., Roberts, A.P., Tamisiea, M.E., Williams, F.,  
329 2014. Sea-level and deep-sea-temperature variability over the past 5.3 million years. *Nature*  
330 508, 477–482.

331 Saito, Y., 1989. Modern storm deposits in the inner shelf and their recurrence intervals, Sendai  
332 Bay, northeast Japan. In: Taira, A., Masuda, F. (Eds.), *Sedimentary facies in the active plate*  
333 *margin*. Terra Scientific Publishing Company, Tokyo, 331–344.

334 Sato, T., Takayama, T., 1992. A stratigraphically significant new species of the calcareous  
335 nannofossil *Reticulofenestra asanoi*. In: Ishizaki, K., Saito, T., (Eds.), Centenary of Japanese  
336 Micropaleontology, Terra Scientific Publishing Company, Tokyo, 457–460.

337 Sclater, J.G., Christie, P.A.F., 1980. Continental stretching: an explanation of the post  
338 Mid-Cretaceous subsidence of the central North Sea basin. *Journal Geophysical Research* 85,  
339 3711–3739.

340 Sosdian, S., Rosenthal, Y., 2009. Deep-sea temperature and ice volume changes across the  
341 Pliocene-Pleistocene climate transitions. *Science* 325, 306–310.

342 Takayama, T., Kato, M., Kudo, T., Sato, T., Kameo, K., 1988. Calcareous microfossil  
343 biostratigraphy of the uppermost Cenozoic formations distributed in the coast of the  
344 Japan Sea, Part 2: Hokuriku sedimentary basin. *Journal of the Japanese Association for*  
345 *Petroleum Technology* 53, 9–27 [Japanese with English abstract].

346 Walker, R.G., Plint, A.G., 1992. Wave- and storm-dominated shallow marine systems. In Walker,  
347 R.G., James, N.P. (Eds). *Facies models: Response to sea level change*. Geological  
348 Association of Canada 219–238.

349 Yu, J., Broecker, W. S., 2010. Comment on “Deep-sea temperature and ice volume changes  
350 across the Pliocene-Pleistocene climate transitions” *Science* 328, 1480c.

351

352

353

354

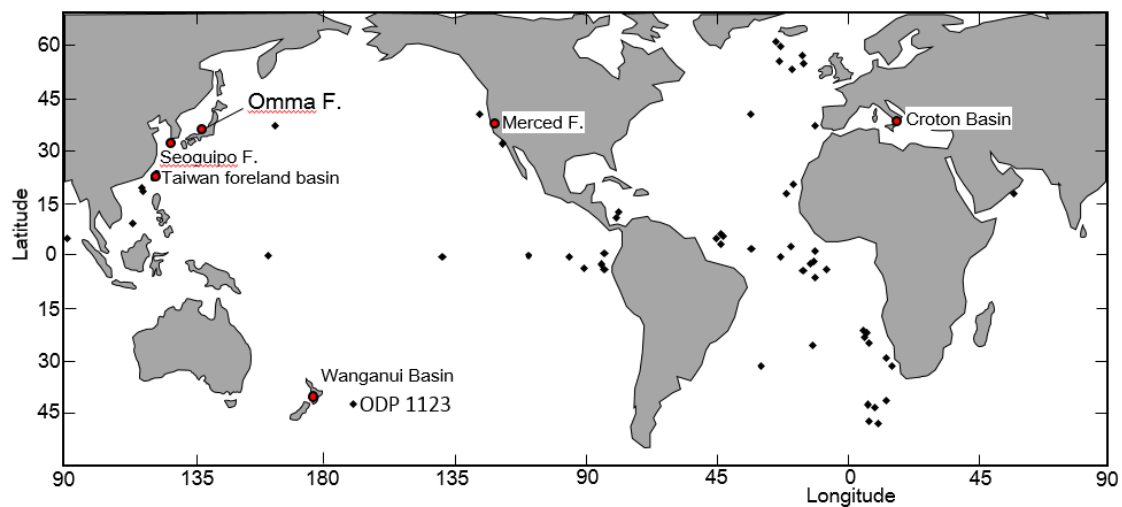
355

356

357

358

359



360

Figure 1 Locations of deep-sea cores (diamond symbols) used in the LR04 “stacked” benthic  $\delta^{18}\text{O}$  record (Lisiecki and Raymo, 2005), location of ODP 1123 (Elderfield et al., 2012), and locations of early Pleistocene shelfal and nearshore sedimentary records (circles).

363

364

365

366

367

368

369

370

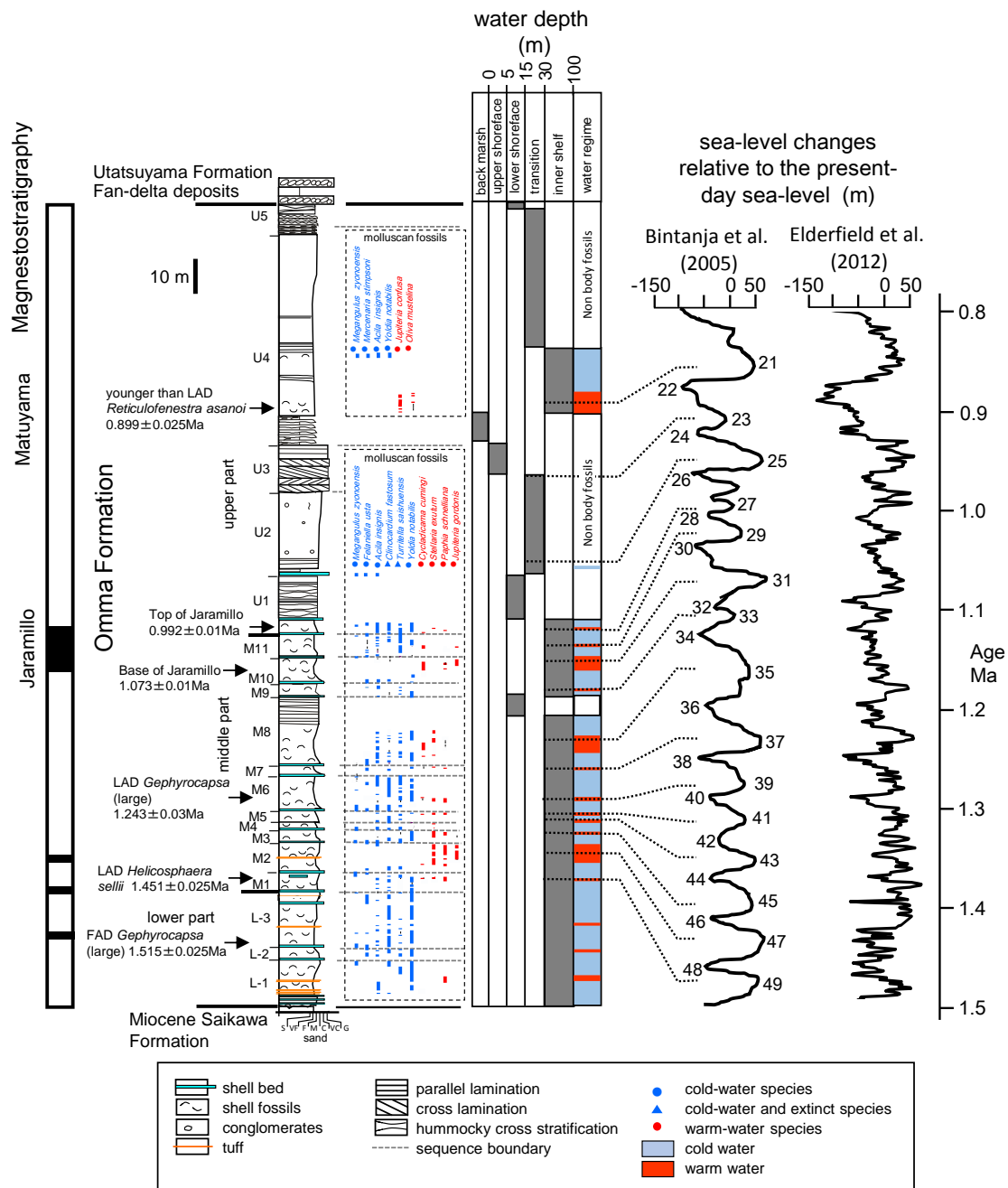
371

372

373

374

375



376

377 Figure 2 Columnar section of the Omma Formation at its type section along the Saikawa River  
 378 at Okuwa. Comparison of water-depth changes reconstructed from the Omma Formation and  
 379 eustatic sea-level changes inferred from geochemical signals of benthic foraminifera in deep-sea  
 380 sediments (Bintanja et al., 2005; Elderfield et al., 2012).